Int. J. Electrochem. Sci., 15 **(2020)** 6135 – 6142, doi: 10.20964/2020.07.65

International Journal of
ELECTROCHEMICAL
SCIENCE
www.electrochemsci.org

Short Communication

Effect of Bagasse Ash Admixture on Corrosion Behavior of Low Carbon Steel Reinforced Concrete in Marine Environment

QingYan Zhang[1,], Hualei Li[2], Hongwei Feng[1], Tao Jiang[1]*

[1] Xinxiang University, *Xinxiang, Henan 453003*, China
[2] Xinxiang Vocational and Technical College, Xinxiang, Henan 453003, China
[*]E-mail: qingyanzhang00@sina.com

Received: 14 March 2020 / *Accepted:* 27 April 2020 / *Published:* 10 June 2020

The effect of bagasse ash (BA) admixture in various concentrations into Portland cement on the electrochemical corrosion resistance of carbon steel reinforced concrete was evaluated by electrochemical impedance spectroscopy and polarization methods during immersion in 3.5 wt% NaCl solution as the marine environment. Reinforced concrete with 10 wt% BA was most effective for enhancing the corrosion resistance of the steel rebar due to the decrease of water absorptivity and chloride ion permeability. The surface morphology of the samples indicated that irregularity and separation structures on the steel rebar were improved by adding BA. The results indicate that the BA as an admixture increases concert durability and prevents the corroding ions from reaching the surface of the steel rebars which can be an alternative material in the development of construction industry.

Keywords: Bagasse ash; Electrochemical corrosion resistance; Low carbon steel rebar; Electrochemical impedance spectroscopy; polarization

1. INTRODUCTION

Reinforced concrete is currently used in major infrastructures such as ports, tunnels, bridges and marine construction [1]. However, its durability can be particularly compromised by corrosion processes [2]. One of the most important causes of damage in reinforcement concrete is chloride-induced corrosion [3]. There are various approaches to prevent corrosion in reinforcement concrete such as epoxy coatings, corrosion inhibitors and cathodic protection [4-6]. However, these techniques are not very effective and expensive.

A partial replacement for Portland cement (PC) through supplementary cementitious materials (SCM) can be another ecological and viable option to prevent corrosion [7]. SCM reduces the permeability and porosity of concrete because of the formation of cementitious compounds through a reaction of pozzolanic with the calcium hydroxide from the cement hydration [8].

Mineral additives are usually used in several applications such as high performance concrete buildings, bridges and off-shore and on-shore structures. Famous mineral additives include fly ash, rice husk ash, and silica fume [9, 10]. The addition of these materials in the concrete production have positive environmental effects and minimizing problems related to its disposal.

Bagasse ash (BA) is a by-product derived from the combustion of bagasse in sugar factories [11]. It is mostly deposited in open dumps which causes pollution and disposal problems. Once the BA is post-treated, it could be utilized as SCM in concrete and mortar mixtures due to its pozzolanic property which develops the concrete microstructure without adverse effects on its mechanical activities [12, 13].

In this case, replacement of fine aggregates can lead to improved durability using pore refinement and enhanced resistance to the diffusion of deleterious agents. A number of studies have found that the possible benefits of BA in decreasing the macro-pores is greater than 0.1 µm and remarkably increasing the resistance to chloride diffusion in SCM [14, 15]. However, the BA influence on durability of concrete structure in terms of corrosion improvement, mainly in combination with SCM is still deficient and unclear. Thus, this study aims to investigate the effect of BA as a partial fine aggregate in corrosion procedure of reinforced PC concrete. In this work, reinforced concrete with different BA contents were assessed by electrochemical characterizations such as corrosion rate and corrosion potential under a marine environment.

2. MATERIALS AND METHOD:

In this study, concrete specimens were cast using different concentrations of bagasse ash (0, 5, 10 and 15%) by weight of cement which were produced with replacement of PC by BA. The chemical compositions of the PC and BA used are shown in Table 1. The PC was mixed with gravel, sand, and water (1.5: 1: 3: 0.5) to prepare concrete structure. The mixed cements were made by a high-speed mixer machine to attain a heterogeneous dispersion. Carbon steel rebars were utilized as a working electrode in electrochemical test.

Table 1. Chemical compositions of the bagasse ash and Portland cement

Parameters	**Portland cement**	**Bagasse ash**
SiO_2 (%)	19.98	51.74
Al_2O_3 (%)	4.74	9.52
Fe_2O_3 (%)	3.02	2.65
CaO (%)	63.53	9.82
MgO (%)	2.04	4.36
K_2O (%)	0.65	9.53
Na_2O (%)	0.27	4.45
SO_3 (%)	2.65	3.42
LOI (%)	3.12	4.51

The chemical composition of the carbon steel rebars was C (0.1 wt%), Si(1.5wt%), Mn(0.83 wt%), Cr(0.06 wt%), Ni(0.1 wt%), Al(0.01 wt%), Cu(0.34wt%), Fe is the balance. Carbon steel reinforcement with a diameter of 1 cm and the length of 6 cm was placed in the cylinder at a cover of 3 cm. Mild steel bars were first immersed in acetone solution and then washed with deionized water.

The open circuit potential of the different samples were periodically performed by a high-impedance voltmeter with 10 MΩ input resistance. A three-electrode electrichemical system, including of the mild steel rebar, graphite and a standard copper/copper sulfate electrode were used as the working, counter and reference electrodes, respectively. All analysis were done in the 3.5% w/w NaCl solution as a simulated marine environment. Electrochemical impedance spectroscopy (EIS, Wuhan CorrTest Instruments Corp., Ltd.) were done at 10 mV amplitude with scanning range of 0.01 Hz to 0.1 MHz. The polarization measurement was done from 250 mV at scanning rate of 1 mV/s. The surface morphologies of the specimens were studied by Zeiss Sigma 300 VP scanning electron microscope (SEM).

3. RESULTS and DISCUSSION

Low carbon steel reinforced concretes were produced with replacement of PC by different concentrations of bagasse ash (BA). Figure 1 indicates corrosion potential of specimens exposed to 3.5 wt% NaCl solution which show that the samples with BA contents more than 5 wt% have a 10% corrosion probability for the whole exposure time, with corrosion potential of larger than -200 mV. Samples with 0 wt% BA revealed an uncertain corrosion from 1 to 6 weeks with the potential values between -300 mV and -200 mV vs. CSE, associated to the initiation of pitting corrosion or small separation of the passive layer [16].

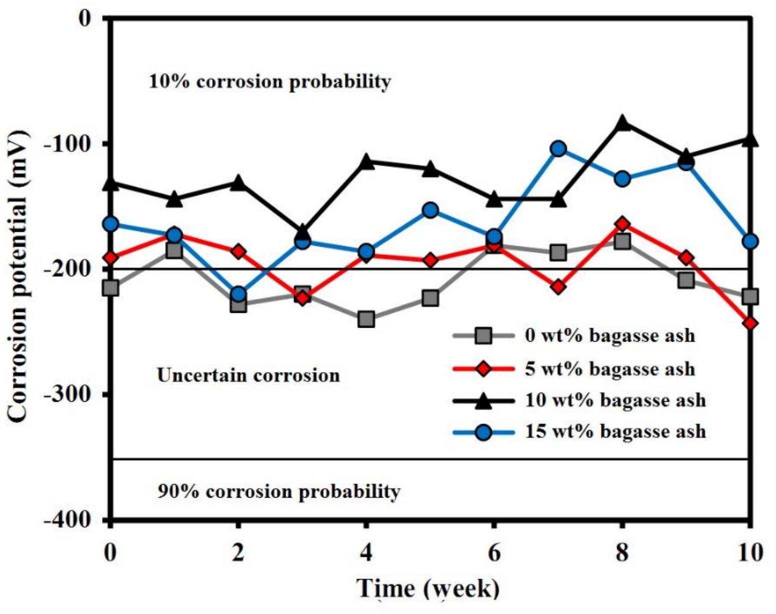

Figure 1. Corrosion potential of steel reinforced concrete produced by replacement of PC by different contents of bagasse ash exposed to 3.5 wt% NaCl solution

The corrosion potential values for 10 wt% BA sample indicated a more stable potential value than the other samples, where their potential values remained completely in 10% corrosion probability region. One of the most important properties of the BA is its significant influence on the durability of concrete [17, 18], which is due to the decrease in calcium hydroxide, solubility of hydration products and change in pore solution.

Figure 2 indicates the polarization curves of low carbon steel rebars in various concrete specimens exposed to 3.5 wt% NaCl environment after five weeks exposure period. The anodic polarization plots were evaluated by passive zones in all steel rebars, indicating that the passive films had obviously been created on the surface of the rebars when they were exposed to 3.5 wt% NaCl solution [19, 20]. Moreover, a considerable shift into a more positive corrosion potential was found which showed that the anodic metal dissolution was efficiently retarded by varying the concrete content [21, 22].

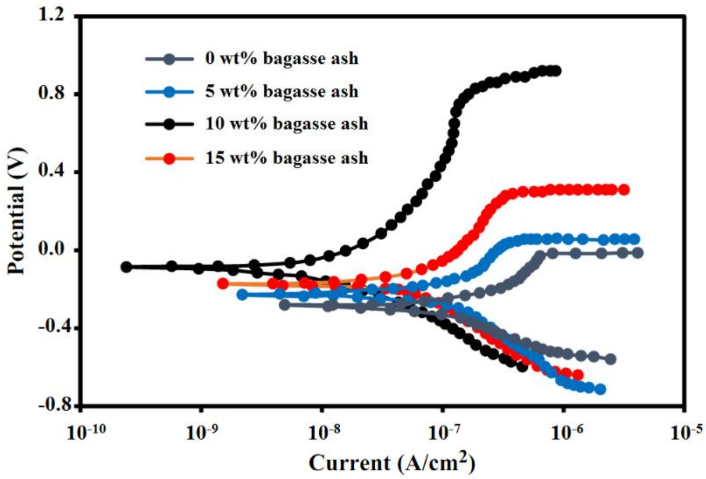

Figure 2. Polarisation curves of low carbon steel rebar in different concrete specimens exposed to 3.5 wt% NaCl environment after five weeks exposure time

Table 2. Fitting results of polarization plots for the carbon steel rebars in 3.5 wt% NaCl solution

Concrete	Corrosion current density	Corrosion potential	β_c ($mVdec^{-1}$)	$-\beta_a$ ($mVdec^{-1}$)
PC	0.231 μA/cm^2	-0.232 V	195	215
5 wt% BA	0.166 μA/cm^2	-0.198 V	196	206
10 wt% BA	0.035 μA/cm^2	-0.116 V	178	238
15 wt% BA	0.093 μA/cm^2	-0.164 V	187	221

The corrosion parameters are shown in table 2 which were attained from the polarization plots in figure 2.

The classification of corrosion can be introduced in four levels proposed by Durar Network Specification [23]. However, the 10 wt% BA sample shows lower corrosion current density than that of the other samples in 3.5 wt% NaCl solution (Table 2). Hence, steel reinforced concretes with BA content more than 5 wt% remained in the passive state throughout the experiment which indicated a high corrosion resistance of low steel rebar in 3.5 wt% NaCl solution.

Furthermore, anodic Tafel slope (β_a) and cathodic Tafel slope (β_c) were determined by the Tafel extrapolation technique which are indicated in table 2. The values of β_a and β_c were changed in different concrete structures. The variation of Tafel slope values may be used to recognise the inhibition mechanism (cathodic or anodic) for carbon steel rebar, the electrolyte concentration, the working electrode composition and the charge transfer coefficient [24].

Given that the BA contents can reduce the porosity and water absorptivity in concrete structure, the corrosion resistance of low carbon steel rebar can be enhanced by addition BA [25, 26]. Thus, the BA replacement aids to promote a reinforced concrete structure that decreases the absorption of chloride rou

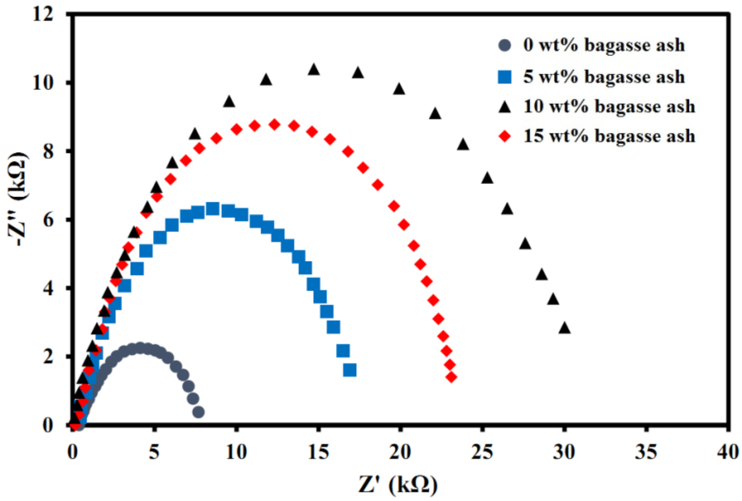

Figure 3. Nyquist plots of low carbon steel rebar in different concrete specimens exposed to 3.5 wt% NaCl environment

EIS technique was used to evaluate the corrosion resistance of low carbon steel rebar embedded into the concretes with various admixtures at 3.5 wt% NaCl solution. Figure 3 shows the Nyquist plots reached by the EIS analysis. The equivalent circuit used to fit EIS data is shown in Figure 4. Where R_s is the solution resistance. Q_1 and R_1 reveal the capacitance and resistance of the coated concrete, respectively. Q_2 and R_2 are the double-layer capacitance and the charge ransfer resistance of steel rebar surface, respectively [27]. The obtained data are shown in Table 3.

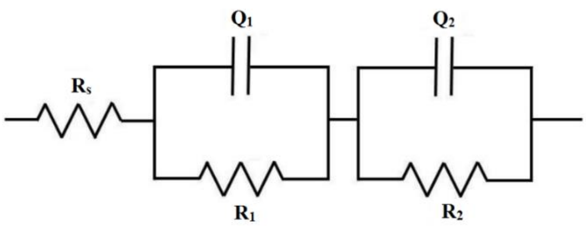

Figure 4. Equivalent circuit model used to fit EIS data

Table 3. The achieved data from the equivalent circuit used to fit EIS data

Concrete	**R_s (Ω)**	**R_1 (kΩ)**	**Q_1(μF cm^{-2})**	**R_2 (kΩ)**	**Q_2(μF cm^{-2})**
PC	23.6	5.25	6.4	7.62	8.3
5 wt% BA	15.8	9.87	3.3	17.68	5.9
10 wt% BA	18.7	20.48	1.7	32.14	2.8
15 wt% BA	21.3	14.36	2.5	23.25	3.7

These results indicate that by the proper replacement of BA in the PC, R_1 increases and Q_2 reduces, which shows an improvement in the stability of the passive film and corrosion resistance on the low carbon steel rebar [28]. Due to the high surface area of the BA, it can form a strong adhesion to hydrated cement, causing a better growth inhibition of the calcium hydroxide [29]. The BA admixtures fill the tiny cracks and capillary pores and ultimately shrink the structure of cement. These agents enhance the corrosion resistance of carbon steel rebars in aggressive solutions. Moreover, comparing Q_2 and Q_1, it was observed that Q_1 was lower than Q_2 in all specimens which had proven that the formation of double and passive layers at the interfaces had high capacitive behavior [30, 31].

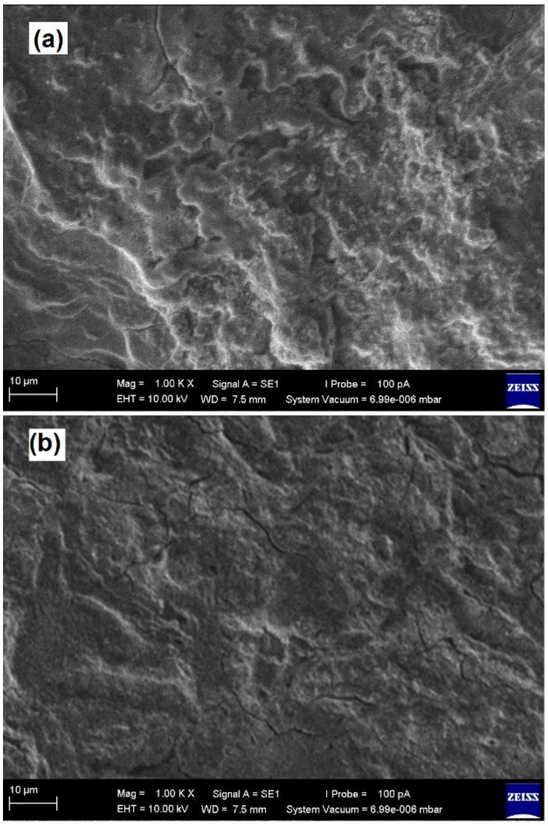

Figure 5. SEM images of carbon steel rebars in different concrets. (a) PC concrete, (b) 10 wt% BA concrete exposed to 3.5 wt% NaCl environment after five weeks exposure time

Figure 5 indicates the surface morphology of carbon steel rebars in different concerts with and without BA, and exposed to 3.5 wt% NaCl environment after five weeks. The irregularity and separation structures were improved by adding BA. Figure 5b shows that the rebar sample containing 10 wt% BA is more uniform than that of the PC sample which are practically in agreement with previous studies reported [32-34]. The BA contains high concentrations of SiO_2 and Al_2O_3, which decrease the hydration heat that caused by the reaction of water-cement [35]. Furthermore, the BA is investigated as a filler, which reduces concrete permeability and increases its durability and prevents the corroding ions from reaching the surface of the steel rebars.

4. CONCLUSIONS

A partial replacement for Portland cement through supplementary cementitious materials can be an ecological and viable option to prevent corrosion. In this work, the effect of BA admixture in various concentrations into Portland cement on the electrochemical corrosion resistance of carbon steel reinforced concrete was evaluated by EIS and polarization methods during immersion in 3.5 wt% NaCl solution as marine environment. Reinforced concrete with 10 wt% BA was the most effective in enhancing the corrosion resistance of the steel rebar due to the decrease of water absorptivity and chloride ion permeability. The surface morphology of the samples indicate that irregularity and separation structures on the steel rebars were improved by adding BA. The 10 wt% BA sample shows lower corrosion current density than that of the other samples in 3.5 wt% NaCl solution. The results indicate that the BA as an admixture increases concert durability and prevents the corroding ions from reaching to the surface of steel rebars which can be an alternative material in the development of construction industry.

References

1. K. Li, D. Zhang, Q. Li and Z. Fan, *Cement and Concrete Research*, 115 (2019) 545.
2. Y. Song, Y. Tian, X. Li, J. Wei, H. Zhang, P.L. Bond, Z. Yuan and G. Jiang, *Water research*, 150 (2019) 392.
3. A. Brenna, S. Beretta, F. Bolzoni, M. Pedeferri and M. Ormellese, *Construction and Building Materials*, 137 (2017) 76.
4. M. Balonis, G. Sant and O.B. Isgor, *Cement and Concrete Composites*, 101 (2019) 15.
5. A.M. Aguirre-Guerrero, R.A. Robayo-Salazar and R.M. de Gutiérrez, *Applied Clay Science*, 135 (2017) 437.
6. H. Karimi-Maleh and O.A. Arotiba, *Journal of colloid and interface science*, 560 (2020) 208.
7. K. Kupwade-Patil, C. De Wolf, S. Chin, J. Ochsendorf, A.E. Hajiah, A. Al-Mumin and O. Büyüköztürk, *Journal of cleaner production*, 177 (2018) 547.
8. G. Girskas and G. Skripkiūnas, *Construction and Building Materials*, 142 (2017) 117.
9. N.S. Msinjili, W. Schmidt, A. Rogge and H.-C. Kühne, *African Journal of Science, Technology, Innovation and Development*, 11 (2019) 417.
10. O.A. Mohamed and O.F. Najm, *Frontiers of Structural and Civil Engineering*, 11 (2017) 406.
11. M. Brindhalakshmi, T. Kayalvizhi and S. Gunasekar, *International Research Journal of Multidisciplinary Technovation*, 1 (2019) 475.
12. M. Keramatikerman, A. Chegenizadeh and S. Terzaghi, *EJGE*, 24 (2019) 1.
13. H. Karimi-Maleh, F. Karimi, M. Alizadeh and A.L. Sanati, *The Chemical Record*, 20 (2019) 1.

14. A. Bahurudeen, K. Wani, M.A. Basit and M. Santhanam, *Journal of Materials in Civil Engineering*, 28 (2016) 04015095.
15. K. Kiran and I.S. Kishore, *International Journal of Civil Engineering and Technology*, 8 (2017) 452.
16. W. Yongqiang, S. Hao, L. Na, X. Yanhao and J. Hemin, *International Journal of Electrochemical Science*, 13 (2018) 9868.
17. P. Rattanachu, W. Tangchirapat and C. Jaturapitakkul, *Journal of Materials in Civil Engineering*, 31 (2019) 04019093.
18. F. Husairi, J. Rouhi, K. Eswar, C.R. Ooi, M. Rusop and S. Abdullah, *Sensors and Actuators A: Physical*, 236 (2015) 11.
19. S. Mundra, M. Criado, S.A. Bernal and J.L. Provis, *Cement and Concrete Research*, 100 (2017) 385.
20. S. Kakooei, H.M. Akil, M. Jamshidi and J. Rouhi, Construction and Building Materials, 27 (2012) 73.
21. M. Talebian, K. Raeissi, M. Atapour, B. Fernández-Pérez, A. Betancor-Abreu, I. Llorente, S. Fajardo, Z. Salarvand, S. Meghdadi and M. Amirnasr, *Corrosion Science*, 160 (2019) 108130.
22. J. Rouhi, M.R. Mahmood, S. Mahmud and R. Dalvand, *Journal of Solid State Electrochemistry*, 18 (2014) 1695.
23. C. Chen, J. Zuo and Y. Wang, *International Journal of Electrochemical Science*, 15 (2020) 1634.
24. W. Shi, R. Ding, X. Li, Q. Xu and E. Liu, *Electrochimica Acta*, 242 (2017) 247.
25. N. Naderi, M. Hashim and J. Rouhi, *International Journal of Electrochemical Science*, 7 (2012) 8481.
26. A. Khodadadi, E. Faghih-Mirzaei, H. Karimi-Maleh, A. Abbaspourrad, S. Agarwal and V.K. Gupta, *Sensors and actuators b: chemical*, 284 (2019) 568.
27. S.B. Aoun, M. Bouklah, K. Khaled and B. Hammouti, *International Journal of Electrochemical Science*, 11 (2016) 7343.
28. S. Kakooei, H.M. Akil, A. Dolati and J. Rouhi, *Construction and Building Materials*, 35 (2012) 564.
29. J. Rouhi, S. Mahmud, S.D. Hutagalung, N. Naderi, S. Kakooei and M.J. Abdullah, *Semiconductor Science and Technology*, 27 (2012) 065001.
30. S. Chakri, I. Frateur, M.E. Orazem, E. Sutter, T. Tran, B. Tribollet and V. Vivier, *Electrochimica Acta*, 246 (2017) 924.
31. H. Karimi-Maleh, C.T. Fakude, N. Mabuba, G.M. Peleyeju and O.A. Arotiba, *Journal of colloid and interface science*, 554 (2019) 603.
32. V.A. Franco-Luján, M.A. Maldonado-García, J.M. Mendoza-Rangel and P. Montes-García, *Construction and Building Materials*, 198 (2019) 608.
33. M.A. Baltazar-Zamora, A. Landa-Sánchez, L. Landa-Ruiz, H. Ariza-Figueroa, P. Gallego-Quintana, A. Ramírez-García, R. Croche and S. Márquez-Montero, *European Journal of Engineering Research and Science*, 5 (2020) 127.
34. R. Asadpour, N. B. Sapari, M. Hasnain Isa, S. Kakooei and K. Uka Orji, *Fibers and Polymers*, 16 (2015) 1830.
35. K. Saranya, M. Santhoshkumar, S. Sathish, S. Gopinath and P. Parimelashwaran, *International Journal of Emerging Technology in Computer Science & Electronics*, 21 (2016) 61.